Published in final edited form as:
Physiology (Bethesda). 2008 October ; 23: 275–285. doi:10.1152/physiol.00019.2008.

The Unique Nature of Mg^{2+} Channels

Andrea S. Moomaw and **Michael E. Maguire**
Department of Pharmacology, School of Medicine, Case Western Reserve University, Cleveland, Ohio

Abstract

Considering the biological abundance and importance of Mg^{2+}, there is a surprising lack of information regarding the proteins that transport Mg^{2+}, the mechanisms by which they do so, and their physiological roles within the cell. The best characterized Mg^{2+} channel to date is the bacterial protein CorA, present in a wide range of bacterial species. The CorA homolog Mrs2 forms the mitochondrial Mg^{2+} channel in all eukaryotes. Physiologically, CorA is involved in bacterial pathogenesis, and the Mrs2 eukaryotic homolog is essential for cell survival. A second Mg^{2+} channel widespread in bacteria is MgtE. Its eukaryotic homologs are the SLC41 family of carriers. Physiological roles for MgtE and its homologs have not been established. Recently, the crystal structures for the bacterial CorA and MgtE Mg^{2+} channels were solved, the first structures of any divalent cation channel. As befits the unique biological chemistry of Mg^{2+}, both structures are unique, unlike that of any other channel or transporter. Although structurally quite different, both CorA and MgtE appear to be gated in a similar manner through multiple Mg^{2+} binding sites in the cytosolic domain of the channels. These sites essentially serve as Mg^{2+} "sensors" of cytosolic Mg^{2+} concentration. Many questions about these channels remain, however, including the molecular basis of Mg^{2+} selectivity and the physiological role(s) of their eukaryotic homologs.

Magnesium

Mg^{2+} is the most abundant divalent cation in living cells. It is present at a total cellular concentration of 15−25 mM in both prokaryotic and mammalian cells (39,53,55). In the cytosol, the majority of Mg^{2+} is bound to ATP and other phosphonucleotides and to multiple enzymes. In all cells, Mg^{2+} serves as an essential structural element for ribosomes and membranes and as a required cofactor for ATP in the catalytic pocket of a multitude of enzymes. In prokaryotes, Mg^{2+} has also been identified as an important regulatory signal essential for virulence (10,70).

The chemistry of divalent magnesium is unique among the biologically important cations. The hydrated radius of Mg^{2+} is ~400 times larger than the dehydrated radius, a much larger difference than that seen with Na^+ and Ca^{2+} (~25-fold) or K^+ (fourfold). Of all biological cations, Mg^{2+} is the most charge dense, holding the waters within its hydration shell tighter by a factor of 10^3–10^4 than do Ca^{2+}, K^+, and Na^{2+} (39). In addition, the hydrated Mg^{2+} cation is more rigid than other cations, always hexacoordinate, and almost always prefers to coordinate with oxygen. Proteins that transport Mg^{2+} must be able to recognize the very large hydrated cation, strip the tightly bound hydration shell from the cation, and only then transport the dehydrated form. These chemical properties of Mg^{2+} thus predict that proteins that recognize and transport Mg^{2+} will be unique (19,36).

E-mail: andrea.moomaw@case.edu.

Mg^{2+} Transport Proteins

The most thoroughly characterized Mg^{2+} transport proteins to date are from prokaryotic sources. Although several genes associated with Mg^{2+} transport in eukaryotic systems have been recently identified (Table 1), this review will focus on the only two divalent cation channels to be crystallized: CorA and MgtE. The first prokaryotic Mg^{2+} transport system identified and cloned was termed *corA* for the Co^{2+} resistance screen by which it was discovered in *Escherichia coli* and *Salmonella enterica* serovar Typhimurium (22,23,44,49, 61). A locus termed *mgt* was also found to be associated with Mg^{2+} transport and eventually shown to encode a P-type ATPase that mediates Mg^{2+} influx with rather than against its electrochemical gradient (22,66-69,72,73). Additional work uncovered another widespread Mg^{2+} influx system in prokaryotes encoded by *mgtE* (65,75). Work from this laboratory has subsequently characterized Mg^{2+} flux mediated by each of these systems.

CorA is an ion channel present in approximately half of the microbial genomes currently sequenced. It mediates the influx of Mg^{2+}, Co^{2+}, and Ni^{2+}; it does not transport Mn^{2+}, Ca^{2+}, Zn^{2+}, or Fe^{2+} (45,66). The eukaryotic homolog of CorA is Mrs2, the Mg^{2+} channel of the inner mitochondrial membrane (3,56).

MgtE, like CorA, is the primary Mg^{2+} transport system in about half of bacterial genomes sequenced to date. A minority of organisms carry both CorA and MgtE. MgtE is able to mediate the flux of Mg^{2+} and Co^{2+}. Ni^{2+} is an inhibitor of MgtE, but, unlike CorA, Ni^{2+} is not transported by MgtE (65,75). The eukaryotic homologs of MgtE are the SLC41 family of solute carriers (77).

The CorA Mg^{2+} Channel

CorA structure

Three independent crystal structures of *Thermotoga maritima* CorA have recently been published with resolutions from 2.9 to 3.9 Å. All three structures give essentially the same picture of an apparent closed form of the channel (9,33,51). CorA is a homopentamer with two transmembrane (TM) segments per monomer (FIGURE 1). Both the amino and carboxytermini are positioned in the cytosol. The large NH_2-terminal cytoplasmic domain structure is formed from a new protein fold, consisting of a seven stranded parallel/anti-parallel β-sheet sandwiched between two sets of α-helices ($\alpha_1\alpha_2\alpha_3$) and ($\alpha_4\alpha_5\alpha_6$). A stalk helix (α_7) links this cytosolic domain to TM1. The NH_2-terminal regions of the stalk helix with part of the α_6 helix form a funnel-like structure opening into the cytosol. The stalk helix extends ~100 Å from the cytoplasm into the membrane, forming the inner wall of the funnel and TM1. At the membrane-cytosol interface, the funnel is relatively narrow in diameter at 5 Å, whereas its cytoplasmic mouth is much wider at 20 Å. Many of the α_6 and α_7 stalk helix residues facing the interior of the funnel are negatively charged or bear hydroxyl groups (FIGURE 2). Since CorA is a homopentamer, this arrangement provides a succession of concentric, negatively charged or polar residues that putatively would interact with Mg^{2+} as it exits the membrane pore.

The membrane domain of CorA is formed by two TM segments per monomer, giving 10 TM segments in total. The helices of TM2 form a ring around the outside of the pore, which is composed solely of TM1 helices in the apparent closed form of the channel (FIGURE 3). A proline and a glycine cause TM1 to kink and taper the pore near the periplasmic surface. Distortion by proline and glycine residues in similar positions is a common property of ion channels (74). The distal portion of TM1 near the periplasm contains the signature sequence of all CorA proteins, YGMNF. A BLAST (2) search with this five-amino acid string returns no hits except CorA. This sequence is absolutely required for CorA function (71). In the homopentamer, the asparagine residues contributed by the YGMNF motif appear to block the

pore at the periplasmic face. They are held in place by stacking interactions between the tyrosine of the YGMNF sequence from one monomer and the phenylalanine of the adjacent monomer's YGMNF sequence.

TM2 lies outside the pore formed by TM1 and returns the carboxy-terminus to the cytosol. The periplasmic loop connecting TM1 and TM2 as well as the last two carboxy-terminal amino acids were not resolved in any of the published crystal structures. A universally conserved feature of CorA is a short six-amino acid cytosolic domain of multiple arginines and/or lysines at the COOH terminus. For example, in *S. typhimurium*, this sequence is KRKNWL, wheras in *T. maritima* it is KKKKWL. Including two conserved lysines on the outside face of the α_7 stalk helix, this places a ring of 25−30 lysines 50 Å in diameter external to the pore and adjacent to the membrane, termed the “basic sphincter” (FIGURE 4). This ring is putatively countered by 50 aspartate and glutamate residues from the membrane proximal halves of helices α_5 and α_6, which are positioned almost perpendicular to the membrane, providing a ring of negative charges just above the basic sphincter termed the willow helices.

Interaction of CorA with Mg^{2+}

The large size of a hydrated Mg^{2+} creates a unique problem for Mg^{2+} transporters in terms of selectivity and transport. The ability of cation hexa ammines to selectively inhibit CorA has suggested the hypothesis that CorA initially interacts with the fully hydrated Mg^{2+} ion (30) since the covalently bound ammine groups mimic the size and shape of a hydrated Mg^{2+} cation (6). In addition, the ability of Co(III) and Ru(III) hexaammines to inhibit CorA indicates that this initial interaction is not based strictly on charge since both divalent and trivalent cations bind to CorA (30).

An obvious candidate for site of initial interaction of the channel with a Mg^{2+} cation is the only part of CorA exposed on the periplasmic face of the membrane, the nine-amino acid loop connecting TM1 and TM2 (33). This loop always contains a significant negative charge as well as the highly conserved MPEL motif. This suggests that the periplasmic loop may act as a selectivity filter. In contrast, Payandeh and Pai's crystal structure (51) modeled this unresolved loop by lengthening TM2 and reducing the loop to seven amino acids. The results of their modeling suggested that the MPEL loop lies roughly parallel to the membrane and thus would be poorly positioned to interact with Mg^{2+} and act as a selectivity filter. Further experiments will be required to determine where Mg^{2+} initially binds to CorA.

The CorA pore is ~40 Å in length. It is noteworthy that none of the almost 800 currently known CorA homologs contains a charged amino acid in either TM1 or TM2. Thus electrostatic interactions are not involved in movement of the most charge dense of all biological cations through the membrane. Indeed mutational analysis of the *S. typhimurium* CorA indicates that it is the backbone carbonyls within the pore that primarily interact with Mg^{2+} during its passage (71). In addition to the constriction formed by the ring of five asparagine residues from the YGMNF motif, two additional sites of pore constriction are apparent, creating a maximum width of 6 Å narrowing to 2.5 Å. The smallest of these constrictions is formed by bulky hydrophobic residues at the cytosol-membrane interface (Leu294 and Met291 in the *T. maritima* CorA). A large hydrophobic residue is conserved at the equivalent of position 294 in CorA homologs. Adjacent to this constriction but outside the pore is the basic sphincter, the lysine/arginine ring formed from the COOH terminus. The combination of positive potential from this ring and pore constriction would appear to provide a formidable barrier to passage of a positive cation.

How does Mg^{2+} pass through all of these barriers? The relative positioning of the positively charged basic sphincter and the negatively charged willow helices suggests an answer (9,33, 51). The electrostatic attraction generated between the basic sphincter and the willow helices

could induce movement of the basic sphincter outward and/or upward further into the cytosol, away from the pore and the block formed by Leu294 and Met291. This would necessitate movement of the α_7 stalk helix since part of the lysine/arginine ring is formed from residues of α_7 near the cytosolic end of the pore. The 100 Å length of the stalk helix provides a very long relatively rigid "lever" through which movements elsewhere in the homopentamer could be transmitted to the pore, thereby opening it. Recent mutational analysis of *T. maritima* CorA by Payandeh et al. (50) supports such a gating role for the willow helices.

Regulation of Mg^{2+} transport

How might movement of the willow helices and basic sphincter be controlled to regulate opening and closing of the channel? The structure from Lunin et al. (33) and that from Payandeh and Pai (51) were solved in the presence of Mg^{2+} and Ca^{2+}, respectively. In both, electron density was detected near residues Asp89 of the α_3 helix and Asp253 of the α_7 stalk helix consistent with cation binding (FIGURE 4). Mg^{2+} bound to this site would stabilize a closed conformation of the protein by associating the NH_2-terminal αβα domain of one monomer with the α_7 stalk helix of the adjacent monomer. Mg^{2+} dissociation from these sites could elicit rotation of the αβα domain of one monomer away from the α_7 helix of the funnel wall (9,33, 51). The movement of the willow helices as part of the αβα domain would presumably exert an attraction on the positively charged basic sphincter residues, relieving the block at the membrane-cytosol interface and allowing the protein to open like an iris. Recent mutational data supports this hypothesis (50). It remains to be definitively demonstrated that the Mg^{2+} ions bound to the cytosolic domain have an actual function in gating. Nonetheless, available data indicate that these bound ions act essentially as sensors of cytosolic Mg^{2+} concentration, thus tightly regulating Mg^{2+} movement through CorA and consequently regulating Mg^{2+} homeostasis.

The CorA superfamily

The CorA protein superfamily is widespread in the Eubacteria with about 800 sequences currently known. Although phylogenetic analysis of the family suggests at least two additional subfamilies in addition to the CorA Mg^{2+} channels (26,27), information on function is available only for the subfamily represented by ZntB, which mediates the efflux of Zn^{2+} (4,80). Given its sequence similarity and identical secondary structure to CorA, it has been hypothesized to have a structure similar to that of CorA (38). This hypothesis has recently been confirmed with solution of the crystal structure of the soluble domain of ZntB from *Vibrio parahaemolyticus* (Tan et al., PDB code 3CK6) and *S. typhimurium* (Maguire et al., unpublished observations). These structures show that ZntB is a funnel-shaped homopentamer assembled almost identically to CorA. Efflux of Zn^{2+} via ZntB would move the cation against the electrochemical gradient. This obviously requires energy, most likely in the form of a counter- or co-transported ion, although this has not been formally shown. Thus the CorA superfamily appears to contain both ion channels and transporters, much like the ClC family of carriers (35,41).

Eukaryotic homologs of CorA include the Mrs2 and Lpe10 inner mitochondrial membrane proteins, which were originally identified as being required for group II intron splicing (3,18, 79). Mrs2 is most homologous to CorA in the membrane domain and exhibits the YGMNF motif. That Mrs2 is a true homolog of CorA has been confirmed by demonstration that Mrs2 can functionally substitute for CorA in prokaryotes and that a prokaryotic CorA can in turn functionally substitute for Mrs2 (3,29,81). The human homolog of Mrs2 has been shown to complement the yeast *mrs2* phenotype (81). *Arabidopsis thaliana* also expresses an Mrs2 homolog that can complement both bacterial *corA* and yeast *mrs2* mutants (31,60).

Mrs2 directly transports Mg^{2+} into the mitochondrion as shown both with MagFura-2, a fluorescent Mg^{2+} indicator dye, (29) and from patch clamping of giant lipid vesicles (56). In

the latter experiments, Mrs2 exhibits a conductance of 150 pS. The involvement of these proteins in group II intron splicing is apparently indirect, as the ribozyme structure involved requires adequate Mg^{2+} concentration for function. Mrs2 is apparently the only Mg^{2+} influx pathway in the mitochondrion. Recent studies involving conditional knock down of the human Mrs2 homolog (*Mrs2L*) show that Mrs2 is necessary for Mg^{2+} uptake in mitochondria as well as maintenance of respiratory complex I. Long-term knockdown of Mrs2 results in apoptosis (52).

The ALR1 and ALR2 eukaryotic homologs of CorA were first identified in a screen testing for resistance to aluminum. Overexpression of either protein confers resistance to Al^{3+} and Ga^{3+} ions (34). These proteins are localized in the yeast plasma membrane, and their expression and turnover via endocytosis is controlled by the Mg^{2+} concentration in the environment (17). Electrophysiological studies of ALR1 provide evidence that ALR1 mediates Mg^{2+} influx (32). Recent work has shown that ALR1 and ALR2 are able to form homo-oligomers and hetero-oligomers (78). ALR2 transports Mg^{2+} rather poorly, possibly because the glutamic acid of the highly conserved MPEL motif in the loop between TM1 and TM2 is replaced by a positively charged arginine. Mutation of this arginine to glutamic acid greatly increased the Mg^{2+} transport capacity of ALR2 (78). The ALR proteins are around 800 amino acids long, much larger than CorA, and have an NH_2-terminal extension that presumably binds trivalent cations. Whether the ALR homologs transport trivalent cations is not known, although the phenotype of increased resistance with their overexpression suggests that they mediate either influx of trivalent cations into a vacuole or their efflux across the plasma membrane.

The MgtE Mg^{2+} Channel

MgtE structure

The crystal structure of the full-length bacterial *Thermus thermophilus* MgtE was recently determined by Hattori et al. (20,21) to a resolution of 3.5 Å (FIGURE 5). In addition, the structure of the cytosolic domain was resolved to 2.3 Å in the presence of Mg^{2+} and to 3.9 Å in the absence of Mg^{2+}. MgtE exists as a homodimer with five transmembrane segments per monomer giving, like CorA, 10 total TM segments. The cytosolic domain is highly acidic and composed of two subdomains. The first, the N domain, is located at the NH_2-terminal region of the cytosolic domain and is a right-handed superhelix with 10 total α-helices in each domain. Pallen and Gophna noted that the N domain is structurally homologous to the soluble domain of FliG, a component motor of the bacterial flagellum (44a). Immediately following the N domain is a tandemly repeated cystathionine-β-synthase (CBS) domain, a known dimerization domain in several transporters (25).

Each monomer has five transmembrane helices. The helices are connected by five loops, designated L0–L4 with the L1 and L4 loops containing short α-helices termed H1b and H4b, respectively (FIGURE 5). The transmembrane domain of each monomer is linked with the cytosolic domain by a connecting helix, which interacts with the TM5, TM2, and H4b helices through both dipole moments and van der Waals forces. The connecting helix of each monomer interacts with and is parallel to the connecting helix of the other monomer. Hydrophobic interactions between the TM domains appear to drive dimerization, which is stabilized by hydrogen bond interactions between highly conserved charged and/or polar residues. As is a general feature of many ion channels, several MgtE TM helices are kinked at either a glycine or proline residue.

The ion-conduction pore of MgtE appears to be formed primarily by the TM2 and TM5 helices. The periplasmic entrance to the pore is formed from residues in the L1 loop. In this loop, the H1b helix is exposed to the periplasm and parallel to the membrane. Immediately following H1b, the continuation of L1 forms an initial nonhelical and highly conserved hydrophobic

portion of TM2. A typical sequence here is VVILA. The entrance to the pore at the periplasmic side is ~15 Å in diameter. The entrance on the cytoplasmic side is ~6 Å in diameter. However, in contrast to the periplasmic end of the pore, the cytosolic end is lined with hydrophilic residues, including a conserved aspartate. This is also in contrast to CorA where not one of the almost 800 homologs now known carries a charged residue in either TM1 or TM2.

Interaction of MgtE with Mg^{2+}

The full-length crystal structure of MgtE was solved in the presence of 40 mM Mg^{2+}. The structure revealed five peaks of electron density on each monomer near conserved acidic residues. Bond angles and bond lengths support the interpretation of these densities as bound Mg^{2+} ions (FIGURE 5). The densities are referred to as Mg1–Mg5 (20). Mg1 is in the ion conducting pore and coordinated with the carboxyl group of the aspartate residue in TM5 and to the carbonyl group of an alanine one turn of the helix away. Mg1 coordination is clearly octahedral with short 2.0 Å bond angles near 90°, which is typical of Mg^{2+}. Mg2 and Mg3 are located ~6 Å apart at the interface of the cytosolic and transmembrane domains. Mg2 is coordinated with one residue of the CBS domain and two residues of the connecting helix. Mg3 coordinates with a residue of the CBS domain, a residue of the connecting helix, and a third residue between TM4 and TM5. These locations suggest that Mg^{2+} ions are involved in positioning the connecting helix for proper interaction with TM5, TM2, and H4b to lock the channel in a closed conformation. Mg4 and Mg5 are ~8 Å apart and appear to connect the N and CBS domains. These Mg^{2+} ions are positioned to fix the connecting helix in place and stabilize the interactions between the N and CBS domains. Mg2-Mg3 and/or Mg4-Mg5 would thus appear to play a role similar to the Mg^{2+} ions bound between monomers in CorA.

Regulation of MgtE

The structure of the N domain and the structure of the CBS domain in the presence and absence of Mg^{2+} are virtually identical. However, the absence of Mg^{2+} from the Mg2-Mg3 and Mg4-Mg5 sites appears to allow the N domain to rotate ~120° away from the CBS domain. The dimerization of the two tandem CBS domains within each monomer is also altered in the absence of Mg^{2+}. The connecting helices unlock and rotate ~20° away from each other. Thus the absence of Mg^{2+} induces marked cytosolic domain flexibility. These movements would disrupt the interaction between the transmembrane domains and the connecting helices, allowing rearrangement of the helices that form the pore and presumably opening the pore (FIGURE 6).

These observations suggest that the cytosolic domain of MgtE acts essentially as a Mg^{2+} sensor, allowing the cytosolic domain to regulate gating of the ion-conducting pore. Similarly in CorA, the Mg^{2+} ions bound between each monomer suggest that the cytosolic domain of CorA acts as a Mg^{2+} sensor. Thus, despite their markedly different structures, CorA and MgtE permeability likely is regulated identically in response to changes in cytosolic Mg^{2+} concentration. Unlike CorA, MgtE exhibits an additional level of regulation by Mg^{2+}. Recently, Mg^{2+} controlled riboswitches have been demonstrated in the promoters of two different classes of Mg^{2+} transporter, the *Bacillus sub-tilis mgtE* and *S.* Typhimurium *mgtA* genes (7,8).

The MgtE superfamily

Phylogenetic analysis of bacterial MgtE proteins appears to indicate a single family (77), unlike CorA, which has two and likely three subfamilies (26,27). MgtE homologs in eukaryotes are represented by the SLC41 family of solute carriers with three members to date (SLC41A1−3). The SLC41 family is homologous to MgtE within the transmembrane domain; however, SLC41 transporters have only a short NH_2-terminal domain that lacks similarity to either the N or CBS domains (77). Furthermore, although they contain 10 TM segments like MgtE, these are the product of a single gene, indicating a tandem fusion during evolution. Both SLC41A1

and SLC41A2 have been expressed in *Xenopus laevis* oocytes and have been shown to generate Mg^{2+} currents (13,14). More detailed characterization has been performed by Kolisek et al. (28) after expression of SLC41A1 in both HEK293 cells and the Mg^{2+} transport-deficient strain of *S.* Typhimurium (22). Interestingly these studies revealed that SLC41A1 functions as a Mg^{2+} efflux system in contrast to the Mg^{2+} influx activity of MgtE. SLC41A2 has been subsequently expressed in TRPM7-deficient DT40 cells by Sahni et al. (54) where it appears to mediate Mg^{2+} influx. It remains to be determined whether SLC41A3 mediates influx or efflux.

SLC41A1 mRNA is highly expressed in heart and testis tissues and to a lesser degree in skeletal muscle, kidney, colon, pancreas, prostate, ovaries, adrenal gland, and thyroid gland (77). Expression is regulated by dietary Mg^{2+}. Mice fed a low magnesium diet for 5 days showed a two- to fourfold increase in SLC41A1 mRNA in kidney, colon, and heart (13). In contrast, expression of SLC41A2 mRNA was not significantly changed in either mouse distal convoluted tubule cells maintained in low magnesium or in kidney tissue isolated from mice kept on low magnesium diets (14). The molecular mechanism and physiological role of SLC41A1 regulation are not known.

Remaining Questions and Future Directions

Although the determination of the crystal structures of CorA and MgtE have provided valuable insight into the function of Mg^{2+} channels, there are still numerous aspects of protein function and physiology that have not been resolved. Some important outstanding questions are explored below.

First, how do CorA and MgtE recognize and differentiate between cations? Each channel is highly selective for Mg^{2+} (66). Other than Co^{2+} and Ni^{2+}, neither transports other common divalent cations such as Fe^{2+} and Ca^{2+}. Moreover, for the most part, no other divalent cations even inhibit Mg^{2+} flux (23,37,46,63,65,75). CorA does not differentiate between divalent and trivalent cations as evidenced by its inhibition by trivalent cation hexaammines (30). The mechanism by which this selectivity occurs is unknown.

The structures of CorA and MgtE present an interesting question in terms of symmetry. How does a pentameric protein bind a cation that is always hexacoordinate without greatly distorting the octahedral configuration of the cation? Which residues does Mg^{2+} coordinate with? With CorA, electrostatic interactions can be ruled out since no CorA homolog has a charged residue in TM1 or TM2. Although some serine and threonine residues appear in TM1 or TM2 of the CorA channel, hydroxyl groups appear to have no role, at least from mutational analysis of the *S.* Typhimurium CorA (71). Thus, in CorA, Mg^{2+} appears to interact primarily if not solely with backbone carbonyls within the pore. Given the pentameric nature of the channel, this raises issues of coordination. Mg^{2+} strongly prefers interaction with oxygens in an octahedral conformation with all bond angles close to 90°. Hexacoordinate binding of Mg^{2+} with backbone carbonyls while maintaining anything close to a 90° bond angle is possible only if Mg^{2+} interacts with a single carbonyl atom at a time, the other sites being filled with water. This would require a very large pore diameter. Since such a large pore diameter would not be particularly selective for any cation over another cation, this consideration in turn suggests either that Mg^{2+} coordination within the CorA pore is distorted markedly from the preferred octahedral configuration or that movement of TM1 somehow allows residues within TM2 to also interact with Mg^{2+}. The former scenario would require a great deal of energy to form and maintain the distorted configuration. It seems more likely that the open form of the channel will involve interaction of Mg^{2+} with residues within TM2, even though the currently available structures of CorA suggest that the pore is formed entirely by TM1.

Like CorA, the outer half of the MgtE pore also appears to be highly hydrophobic in virtually all homologs, again suggesting Mg^{2+} interaction with backbone carbonyls. In contrast to CorA however, the inner half of the pore contains a single negatively charged residue, usually an aspartate. In the homodimer, this results in two carboxyl groups that interact with Mg^{2+}, as shown in the crystal structure. Nevertheless, sequence alignments of the hundreds of MgtE homologs currently known indicate that this conserved aspartate is likely the only charged or polar residue within the pore. In both CorA and MgtE, therefore, the primary interaction of Mg^{2+} within the pore is with backbone carbonyls. In MgtE, with its homodimeric structure, this would provide two cognate carbonyl groups spaced 180° apart all through the pore thus readily satisfying Mg^{2+}'s preference for rather rigid 90° bond angles. This preference for 90° bond angles is also satisfied in the binding of Mg1 within the MgtE pore to the carboxyl groups of the two aspartate residues and the carbonyls of the adjacent alanine residues of the dimer, leaving two positions to be filled by waters.

Gating of the CorA and MgtE Mg^{2+} is also unknown. Both structures contain Mg^{2+} ions bound within the cytosolic domain of the channel with a potential to regulate conformation and thus activity. The cation-free crystal structures of the soluble domains, compared with their structures in the presence of cation, clearly suggest that association and dissociation of these bound Mg^{2+} ions has marked effects on the structure and positioning of the cytosolic domain relative to the membrane domain. In the intact channels, these changes presumably are carried to the membrane domain, largely by the α_7 helices of CorA or the connecting helices of MgtE. Although it seems very likely that such regulation via the Mg^{2+} bound to the cytosolic domain of each channel would be physiologically relevant, this remains to be demonstrated.

Another obvious question is to what extent these Mg^{2+} channel structures can provide insight into the structures of Ca^{2+} or other divalent cation channels. We would argue that this is unlikely due to the differences in the chemistry of Mg^{2+} compared with Ca^{2+} and other divalent cations. Independent of structure, however, regulation of divalent cation channels by divalent cation bound to the cytosolic domain could well be a common feature.

Finally, the apparent function of the CorA paralog ZntB is to mediate efflux of Zn^{2+} rather than the influx of Mg^{2+} (80). The recent deposition of coordinates for the structure of the ZntB soluble domain and our own unpublished structural data on ZntB (see above) clearly show that CorA and ZntB share a quite similar architecture. However, the cation binding sites of Mg^{2+} on CorA and Zn^{2+} on ZntB must be different despite similar protein structures. Zn^{2+} has to initially bind to one or more sites within the cytosolic domain before passage out through the pore. Given the current CorA structures, Mg^{2+} must bind either to the external loop between TM1 and TM2 or to residues at the periplasmic end of TM1. In contrast, Zn^{2+} would not need to interact with similar residues at the external end of the pore since this would only impede flux. This is evident in the sequence of the short loop between TM1 and TM2. In CorA, this loop is always composed of large bulky residues, several of which are charged. This loop in ZntB homologs contains little or no charge and is composed largely of smaller residues including three or even four glycines. Moreover, since energy would be required for Zn^{2+} efflux, a counterion would be required, most likely Na^+ or H^+, with unknown stoichiometry. The CorA Mg^{2+} channel requires only a single ion permeation pathway. With ZntB, although H^+ or Na^+ passage could and likely does share some part of the Zn^{2+} pathway, there must be some difference in the routes for each ion. This same issue arises, for example, with the various chloride transporters, some of which are channels and some of which are Cl^-/H^+ symporters (35,41).

The physiological roles of the CorA and MgtE families of Mg^{2+} channels/carriers in both prokaryotes and eukaryotes remain largely unexplored. In bacteria, mutation of CorA attenuates virulence of *S.* Typhimurium (47,48), and loss of MgtE reduces biofilm formation

and motility in another pathogen *Aeromonas hydrophila* (40). Thus these Mg^{2+} channels appear important for virulence. The molecular basis for these effects is not yet known. In mammals, diseases of Mg^{2+} homeostasis linked to Mrs2 (CorA) or SLC41A1 (MgtE) have not been identified to date. Nonetheless, regulation of SLC41 by Mg^{2+} and conditional knockdown of Mrs2 suggest that these Mg^{2+} transporters have significant roles in the homeostasis of Mg^{2+} in eukaryotes. Their regulation suggests the likelihood that mutations causing human disease will be identified, similar to Mg^{2+} deficiency syndromes (1,24) elicited by mutations in the claudin-16 (paracellin-1) and claudin-19 (62), NIPA1 (11), and TRPM6 (58) Mg^{2+} transport systems.

Regarding the MgtE family, we do not yet know what cellular membranes contain the various SLC41 homologs. With regard to the direction of Mg^{2+} flux, SLC41A1 apparently mediates only Mg^{2+} efflux as demonstrated by Kolisek et al. (28). Although SLC41A2 mediates Mg^{2+} influx as demonstrated by Sahni et al. (54), it is not known whether it can mediate efflux. The direction of flux for SLC41A3 is completely unexplored. The SLC41 family members also appear likely to have accessory proteins in the cytosol since they have very short NH_2 termini (28). Although more data exists concerning the mitochondrial homolog Mrs2, many questions regarding its function in the cell also remain. Recent data from Mrs2 knockdown experiments indicates involvement in apoptosis (52). Is this involvement due simply to loss of Mg^{2+} when the channel is not present, or is Mrs2 an active participant in the mitochondrial apoptosis pathway? Likewise, there is also nothing known about the role or regulation of the numerous Mrs2 and ALR proteins that are expressed by plants.

Determination of the structures of the CorA and MgtE Mg^{2+} channels has provided valuable insight into the mechanism by which Mg^{2+} moves across membranes. Befitting the unique chemistry of Mg^{2+}, neither channel has similarity to other known channels or transporters. Nonetheless, although important, solution of their structures provides little information about their functional role(s). Data about the physiology relevant to specific Mg^{2+} transport systems is sorely lacking and must be obtained for a complete picture of Mg^{2+} homeostasis to be synthesized.

References

1. Alexander RT, Hoenderop JG, Bindels RJ. Molecular determinants of magnesium homeostasis: insights from human disease. J Am Soc Nephrol 2008;19:1451–1458. [PubMed: 18562569]
2. Altschul SF, Gish W, Miller W, Myers EW, Lipman DJ. Basic local alignment search tool. J Mol Biol 1990;215:403–410. [PubMed: 2231712]
3. Bui DM, Gregan J, Jarosch E, Ragnini A, Schweyen RJ. The bacterial magnesium transporter CorA can functionally substitute for its putative homologue Mrs2p in the yeast inner mitochondrial membrane. J Biol Chem 1999;274:20438–20443. [PubMed: 10400670]
4. Caldwell AM, Smith RL. Membrane topology of the ZntB efflux system of Salmonella enterica serovar Typhimurium. J Bacteriol 2003;185:374–376. [PubMed: 12486076]
5. Chubanov V, Gudermann T, Schlingmann KP. Essential role for TRPM6 in epithelial magnesium transport and body magnesium homeostasis. Pflügers Arch 2005;451:228–234.
6. Cowan JA. Metallobiochemistry of RNA. $Co(NH_3)_6^{3+}$ as a probe for Mg^{2+}(aq) binding sites. J Inorg Biochem 1993;49:171–175. [PubMed: 7679435]
7. Cromie MJ, Shi Y, Latifi T, Groisman EA. An RNA sensor for intracellular Mg^{2+}. Cell 2006;125:71–84. [PubMed: 16615891]
8. Dann CE III, Wakeman CA, Sieling CL, Baker SC, Irnov I, Winkler WC. Structure and mechanism of a metal-sensing regulatory RNA. Cell 2007;130:878–892. [PubMed: 17803910]
9. Eshaghi S, Niegowski D, Kohl A, Martinez MD, Lesley SA, Nordlund P. Crystal structure of a divalent metal ion transporter CorA at 2.9 angstrom resolution. Science 2006;313:354–357. [PubMed: 16857941]

10. Garcia-Vescovi E, Soncini FC, Groisman EA. Mg^{2+} as an extracellular signal: environmental regulation of *Salmonella* virulence. Cell 1996;84:165–174. [PubMed: 8548821]
11. Goytain A, Hines RM, El-Husseini A, Quamme GA. NIPA1(SPG6), the basis for autosomal dominant form of hereditary spastic paraplegia, encodes a functional Mg^{2+} transporter. J Biol Chem 2007;282:8060–8068. [PubMed: 17166836]
12. Goytain A, Quamme GA. Functional characterization of ACDP2 (ancient conserved domain protein), a divalent metal transporter. Physiol Genomics 2005;22:382–389. [PubMed: 15899945]
13. Goytain A, Quamme GA. Functional characterization of human SLC41A1, a Mg^{2+} transporter with similarity to prokaryotic MgtE Mg^{2+} transporters. Physiol Genomics 2005;21:337–342. [PubMed: 15713785]
14. Goytain A, Quamme GA. Functional characterization of the human solute carrier, SLC41A2. Biochem Biophys Res Commun 2005;330:701–705. [PubMed: 15809054]
15. Goytain A, Quamme GA. Identification and characterization of a novel mammalian Mg^{2+} transporter with channel-like properties. BMC Genomics 2005;6:48. [PubMed: 15804357]
16. Goytain A, Quamme GA. Identification and characterization of a novel family of membrane magnesium transporters, MMgT1 and MMgT2. Am J Physiol Cell Physiol 2008;294:C495–C502. [PubMed: 18057121]
17. Graschopf A, Stadler JA, Hoellerer MK, Eder S, Sieghardt M, Kohlwein SD, Schweyen RJ. The yeast plasma membrane protein Alr1 controls Mg^{2+} homeostasis and is subject to Mg^{2+}-dependent control of its synthesis and degradation. J Biol Chem 2001;276:16216–16222. [PubMed: 11279208]
18. Gregan J, Bui DM, Pillich R, Fink M, Zsurka G, Schweyen RJ. The mitochondrial inner membrane protein Lpe10p, a homologue of Mrs2p, is essential for magnesium homeostasis and group II intron splicing in yeast. Mol Gen Genet 2001;264:773–781. [PubMed: 11254124]
19. Grubbs RD, Maguire ME. Magnesium as a regulatory cation: criteria and evaluation. Magnesium 1987;6:113–127. [PubMed: 3306178]
20. Hattori M, Tanaka Y, Fukai S, Ishitani R, Nureki O. Crystal structure of the MgtE Mg^{2+} transporter. Nature 2007;448:1072–1075. [PubMed: 17700703]
21. Hattori M, Tanaka Y, Fukai S, Ishitani R, Nureki O. Crystallization and preliminary X-ray diffraction analysis of the full-length Mg^{2+} transporter MgtE. Acta Crystallogr Sect F Struct Biol Cryst Commun 2007;63:682–684.
22. Hmiel SP, Snavely MD, Florer JB, Maguire ME, Miller CG. Magnesium transport in *Salmonella typhimurium*: genetic characterization and cloning of three magnesium transport loci. J Bacteriol 1989;171:4742–4751. [PubMed: 2548998]
23. Hmiel SP, Snavely MD, Miller CG, Maguire ME. Magnesium transport in *Salmonella typhimurium*: characterization of magnesium influx and cloning of a transport gene. J Bacteriol 1986;168:1444–1450. [PubMed: 3536881]
24. Hoenderop JG, Bindels RJ. Calciotropic and magnesiotropic TRP channels. Physiology 2008;23:32–40. [PubMed: 18268363]
25. Ignoul S, Eggermont J. CBS domains: structure, function, and pathology in human proteins. Am J Physiol Cell Physiol 2005;289:C1369–C1378. [PubMed: 16275737]
26. Kehres DG, Lawyer CH, Maguire ME. The CorA magnesium transporter gene family. Microbial Comp Genomics 1998;43:151–169.
27. Knoop V, Groth-Malonek M, Gebert M, Eifler K, Weyand K. Transport of magnesium and other divalent cations: evolution of the 2-TM-GxN proteins in the MIT superfamily. Mol Genet Genomics 2005;274:205–216. [PubMed: 16179994]
28. Kolisek M, Launay P, Beck A, Sponder G, Serafini N, Brenkus M, Froschauer EM, Martens H, Fleig A, Schweigel M. SLC41A1 is a novel mammalian Mg^{2+} carrier. J Biol Chem 2008;283:16235–16247. [PubMed: 18367447]
29. Kolisek M, Zsurka G, Samaj J, Weghuber J, Schweyen RJ, Schweigel M. Mrs2p is an essential component of the major electrophoretic Mg^{2+} influx system in mitochondria. EMBO J 2003;22:1235–1244. [PubMed: 12628916]
30. Kucharski LM, Lubbe WJ, Maguire ME. Cation hexaammines are selective and potent inhibitors of the CorA magnesium transport system. J Biol Chem 2000;275:16767–16773. [PubMed: 10748031]

31. Li L, Tutone AF, Drummond RS, Gardner RC, Luan S. A novel family of magnesium transport genes in *Arabidopsis*. Plant Cell 2001;13:2761–2775. [PubMed: 11752386]
32. Liu GJ, Martin DK, Gardner RC, Ryan PR. Large Mg^{2+}-dependent currents are associated with the increased expression of ALR1 in *Saccharomyces cerevisiae*. FEMS Microbiol Lett 2002;213:231–237. [PubMed: 12167543]
33. Lunin VV, Dobrovetsky E, Khutoreskaya G, Zhang R, Joachimiak A, Doyle DA, Bochkarev A, Maguire ME, Edwards AM, Koth CM. Crystal structure of the CorA Mg^{2+} transporter. Nature 2006;440:833–837. [PubMed: 16598263]
34. MacDiarmid CW, Gardner RC. Overexpression of the Saccharomyces cerevisiae magnesium transport system confers resistance to aluminum ion. J Biol Chem 1998;273:1727–1732. [PubMed: 9430719]
35. Maduke M, Miller C, Mindell JA. A decade of CLC chloride channels: structure, mechanism, and many unsettled questions. Annu Rev Biophys Biomol Struct 2000;29:411–438. [PubMed: 10940254]
36. Maguire ME. Magnesium: a regulated and regulatory cation. Met Ions Biol Syst 1990;26:135–153.
37. Maguire ME. Magnesium transporters: properties, regulation and structure. Front Biosci 2006;11:3149–3163. [PubMed: 16720382]
38. Maguire ME. The structure of the CorA magnesium transporter, a divalent cation channel. Curr Opin Struct Biol 2006;4:432–438. [PubMed: 16828282]
39. Maguire ME, Cowan JA. Mg^{2+} chemistry and biochemistry. Biometals 2002;15:203–210. [PubMed: 12206387]
40. Merino S, Gavin R, Altarriba M, Izquierdo L, Maguire ME, Tomas JM. The MgtE Mg^{2+} transport protein is involved in *Aeromonas hydrophila* adherence. FEMS Microbiol Lett 2001;198:189–195. [PubMed: 11430413]
41. Mindell JA, Maduke M. ClC chloride channels. Genome Biol 2001;2:3003.
42. Monteilh-Zoller MK, Hermosura MC, Nadler MJ, Scharenberg AM, Penner R, Fleig A. TRPM7 provides an ion channel mechanism for cellular entry of trace metal ions. J Gen Physiol 2003;121:49–60. [PubMed: 12508053]
43. Nadler MJ, Hermosura MC, Inabe K, Perraud AL, Zhu Q, Stokes AJ, Kurosaki T, Kinet JP, Penner R, Scharenberg AM, Fleig A. LTRPC7 is a Mg ATP-regulated divalent cation channel required for cell viability. Nature 2001;411:590–595. [PubMed: 11385574]
44. Nelson DL, Kennedy EP. Magnesium transport in *Escherichia coli*. Inhibition by cobaltous ion. J Biol Chem 1971;246:3042–3049. [PubMed: 4928897]
44a. Pallen, MF.; Gophna, U. Bacterial flagella and type III secretion: case studies in the evolution of complexity.. In: Volff, JN., editor. Gene and Protein Evolution. Genome Dyn. Vol. 3. Karger; Basel: 2007. p. 30-47.
45. Papp KM, Maguire ME. The CorA Mg^{2+} transporter does not transport Fe^{2+}. J Bacteriol 2004;186:7653–7658. [PubMed: 15516579]
46. Papp KM, Maguire ME. The CorA Mg^{2+} transporter does not transport Fe^{2+}. J Bacteriol 2004;186:7653–7658. [PubMed: 15516579]
47. Papp-Wallace KM, Maguire ME. Regulation of CorA Mg^{2+} channel function affects the virulence of *Salmonella enterica* serovar Typhimurium. J Bacteriology 2008;190:6509–6516.
48. Papp-Wallace KM, Nartea M, Kehres DG, Porwollik S, McClelland M, Libby SJ, Fang FC, Maguire ME. The CorA Mg^{2+} channel is required for the virulence of *Salmonella enterica* serovar Typhimurium. J Bacteriology 2008;190:6517–6523.
49. Park MH, Wong BB, Lusk JE. Mutants in three genes affecting transport of magnesium in *Escherichia coli*: physiology and genetics. J Bacteriol 1976;126:1096–1103. [PubMed: 780341]
50. Payandeh J, Li C, Ramjeesingh M, Poduch E, Bear CE, Pai EF. Probing structure-function relationships and gating mechanisms in the CorA Mg^{2+} transport system. J Biol Chem 2008;283:11721–11733. [PubMed: 18276588]
51. Payandeh J, Pai EF. A structural basis for Mg^{2+} homeostasis and the CorA translocation cycle. EMBO J 2006;25:3762–3773. [PubMed: 16902408]
52. Piskacek M, Zotova L, Zsurka G, Schweyen RJ. Conditional knock-down of hMRS2 results in loss of mitochondrial Mg^{2+} uptake and cell death. J Cell Mol Med. In press

53. Romani A, Scarpa A. Regulation of cell magnesium. Arch Biochem Biophys 1992;298:1–12. [PubMed: 1524417]
54. Sahni J, Nelson B, Scharenberg AM. SLC41A2 encodes a plasma-membrane Mg^{2+} transporter. Biochem J 2007;401:505–513. [PubMed: 16984228]
55. Scarpa A, Brinley FJ. In situ measurements of free cytosolic magnesium ions. Fed Proc 1981;40:2646–2652. [PubMed: 7286245]
56. Schindl R, Weghuber J, Romanin C, Schweyen RJ. Mrs2p forms a high conductance Mg^{2+} selective channel in mitochondria. Biophys J 2007;93:3872–3883. [PubMed: 17827224]
57. Schlingmann KP, Gudermann T. A critical role of TRPM channel-kinase for human magnesium transport. J Physiol 2005;566:301–308. [PubMed: 15845589]
58. Schlingmann KP, Weber S, Peters M, Niemann NL, Vitzthum H, Klingel K, Kratz M, Haddad E, Ristoff E, Dinour D, Syrrou M, Nielsen S, Sassen M, Waldegger S, Seyberth HW, Konrad M. Hypomagnesemia with secondary hypocalcemia is caused by mutations in TRPM6, a new member of the TRPM gene family. Nat Genet 2002;31:166–170. [PubMed: 12032568]
59. Schmitz C, Perraud AL, Johnson CO, Inabe K, Smith MK, Penner R, Kurosaki T, Fleig A, Scharenberg AM. Regulation of vertebrate cellular Mg^{2+} homeostasis by TRPM7. Cell 2003;114:191–200. [PubMed: 12887921]
60. Schock I, Gregan J, Steinhauser S, Schweyen R, Brennicke A, Knoop V. A member of a novel *Arabidopsis thaliana* gene family of candidate Mg^{2+} ion transporters complements a yeast mitochondrial group II intron-splicing mutant. Plant J 2000;24:489–501. [PubMed: 11115130]
61. Silver S. Active transport of magnesium in *Escherichia coli*. Proc Natl Acad Sci USA 1969;62:764–771. [PubMed: 4895213]
62. Simon DB, Lu Y, Choate KA, Velazquez H, Al-Sabban E, Praga M, Casari G, Bettinelli A, Colussi G, Rodriguez-Soriano J, McCredie D, Milford D, Sanjad S, Lifton RP. Paracellin-1, a renal tight junction protein required for paracellular Mg^{2+} resorption. Science 1999;285:103–106. [PubMed: 10390358]
63. Smith RL, Banks JL, Snavely MD, Maguire ME. Sequence and topology of the CorA magnesium transport systems of *Salmonella typhimurium* and *Escherichia coli*. Identification of a new class of transport protein. J Biol Chem 1993;268:14071–14080. [PubMed: 8314774]
64. Smith RL, Kaczmarek ML, Kucharski LM, Maguire ME. Magnesium transport in *Salmonella typhimurium*: induction of *mgtA* and *mgtCB* expression during invasion of epithelial and macrophage cells. Microbiology 1998;144:1835–1843. [PubMed: 9695916]
65. Smith RL, Thompson LJ, Maguire ME. Cloning and characterization of *mgtE*, a putative new class of Mg^{2+} transporter from *Bacillus firmus* OF4. J Bacteriol 1995;177:1233–1238. [PubMed: 7868596]
66. Snavely MD, Florer JB, Miller CG, Maguire ME. Magnesium transport in *Salmonella typhimurium*: $^{28}Mg^{2+}$ transport by the CorA, MgtA, and MgtB systems. J Bacteriol 1989;171:4761–4766. [PubMed: 2670893]
67. Snavely MD, Florer JB, Miller CG, Maguire ME. Magnesium transport in *Salmonella typhimurium*: expression of cloned genes for three distinct Mg^{2+} transport systems. J Bacteriol 1989;171:4752–4760. [PubMed: 2548999]
68. Snavely MD, Gravina SA, Cheung TT, Miller CG, Maguire ME. Magnesium transport in *Salmonella typhimurium*: regulation of *mgtA* and *mgtB* expression. J Biol Chem 1991;266:824–829. [PubMed: 1898738]
69. Snavely MD, Miller CG, Maguire ME. The *mgtB* Mg^{2+} transport locus of *Salmonella typhimurium* encodes a P-type ATPase. J Biol Chem 1991;266:815–823. [PubMed: 1824701]
70. Soncini FC, Garcia VE, Solomon F, Groisman EA. Molecular basis of the magnesium deprivation response in *Salmonella typhimurium*: identification of PhoP-regulated genes. J Bacteriol 1996;178:5092–5099. [PubMed: 8752324]
71. Szegedy MA, Maguire ME. The CorA Mg^{2+} transport protein of *Salmonella typhimurium*. Mutagenesis of conserved residues in the second membrane domain. J Biol Chem 1999;274:36973–36979. [PubMed: 10601252]
72. Tao T, Grulich PF, Kucharski LM, Smith RL, Maguire ME. Magnesium transport in *Salmonella typhimurium*: biphasic time and magnesium dependence of the transcription of the *mgtA* and *mgtCB* loci. Microbiology 1998;144:655–664. [PubMed: 9534236]

73. Tao T, Snavely MD, Farr SG, Maguire ME. Magnesium transport in *Salmonella typhimurium: mgtA* encodes a P-type ATPase and is regulated by Mg^{2+} in a manner similar to that of the *mgtB* P-type ATPase. J Bacteriol 1995;177:2654–2662. [PubMed: 7751273]
74. Tieleman DP, Shrivastava IH, Ulmschneider MR, Sansom MS. Proline-induced hinges in transmembrane helices: possible roles in ion channel gating. Proteins 2001;44:63–72. [PubMed: 11391769]
75. Townsend DE, Esenwine AJ, George J III, Bross D, Maguire ME, Smith RL. Cloning of the *mgtE* Mg^{2+} transporter from *Providencia stuartii* and the distribution of *mgtE* in the eubacteria. J Bacteriol 1995;177:5350–5354. [PubMed: 7665526]
76. Voets T, Nilius B, Hoefs S, van der Kemp AW, Droogmans G, Bindels RJ, Hoenderop JG. TRPM6 forms the Mg^{2+} influx channel involved in intestinal and renal Mg^{2+} absorption. J Biol Chem 2004;279:19–25. [PubMed: 14576148]
77. Wabakken T, Rian E, Kveine M, Aasheim HC. The human solute carrier SLC41A1 belongs to a novel eukaryotic subfamily with homology to prokaryotic MgtE Mg^{2+} transporters. Biochem Biophys Res Commun 2003;306:718–724. [PubMed: 12810078]
78. Wachek M, Aichinger MC, Stadler JA, Schweyen RJ, Graschopf A. Oligomerization of the Mg^{2+}-transport proteins Alr1p and Alr2p in yeast plasma membrane. FEBS J 2006;273:4236–4249. [PubMed: 16903865]
79. Wiesenberger G, Waldherr M, Schweyen RJ. The nuclear gene MRS2 is essential for the excision of group II introns from yeast mitochondrial transcripts in vivo. J Biol Chem 1992;267:6963–6969. [PubMed: 1551905]
80. Worlock AJ, Smith RL. ZntB Is a Novel Zn^{2+} Transporter in *Salmonella enterica* Serovar Typhimurium. J Bacteriol 2002;184:4369–4373. [PubMed: 12142406]
81. Zsurka G, Gregan J, Schweyen RJ. The human mitochondrial Mrs2 protein functionally substitutes for its yeast homologue, a candidate magnesium transporter. Genomics 2001;72:158–168. [PubMed: 11401429]

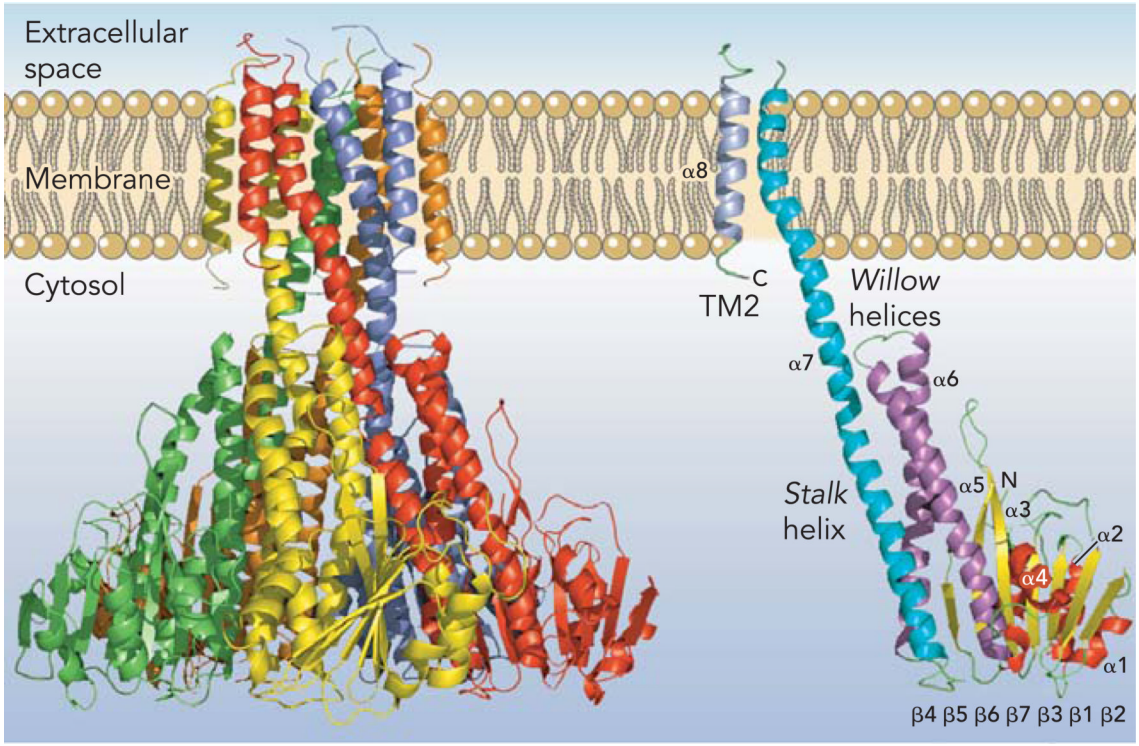

FIGURE 1. CorA Mg^{2+} channel

A: CorA Mg^{2+} channel. The homopentamer is shown from the side with each of the five monomers in a different color. The extracellular space (periplasm) is at *top*. *B*: a single monomer is shown with TM2/α_8 in gray, TM1/α_7 in blue, the willow helices (α_5 and α_6) in purple, the β-sheet (β_1-β_7) in yellow, and the remaining helices (α_1, α_2, α_3) in red.

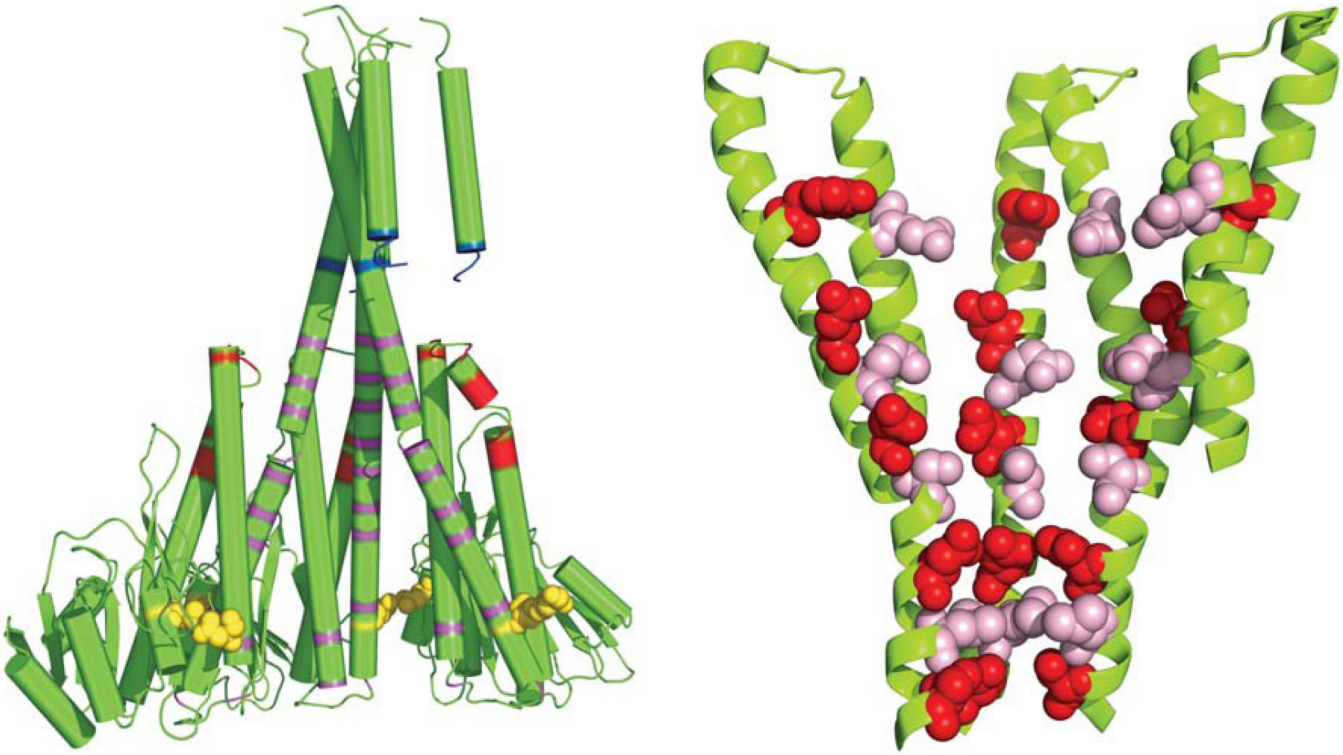

FIGURE 2. Cytosolic charged domains of CorA

A: cartoon view of charged residues in the CorA cytosolic domain. The CorA Mg^{2+} channel of *T. maritima* is shown in cartoon form in green with two monomers removed for clarity. Lysine residues 284, 292, and 346−349 shown in blue comprise the "basic sphincter." Aspartate and glutamate residues at the membrane proximal ends of the willow helices are shown in red (D189, D190, E191, D193, E196, E197, E198, E201, E204, and E206). Charged and hydroxyl-bearing residues that line the pore are shown in magenta (E230, S233, D238, E246, Y255, D263, E266, D270, S273, D277, S280, and S284). Aspartates 89 and 253, which bind a Mg^{2+} ion between adjacent monomers, are shown as yellow spheres. An alternative view is also shown in Figure 4. *B*: cartoon view of charged residues lining the interior face of the funnel of CorA. The cytosolic portions of most of the α_6 and α_7/stalk helices of the *T. maritima* CorA are shown in green. Two of the five monomers have been removed for clarity to allow better visualization. The charged residues that line the inner wall of the funnel formed by α_6 and α_7 are represented as spheres with alternate rings in red (from bottom of funnel: S284, D277, D270, D263, and Y255) and pink (from bottom of funnel: S280, S273, E266, and E230). Residues S233, D238, and E246 are not colored for clarity.

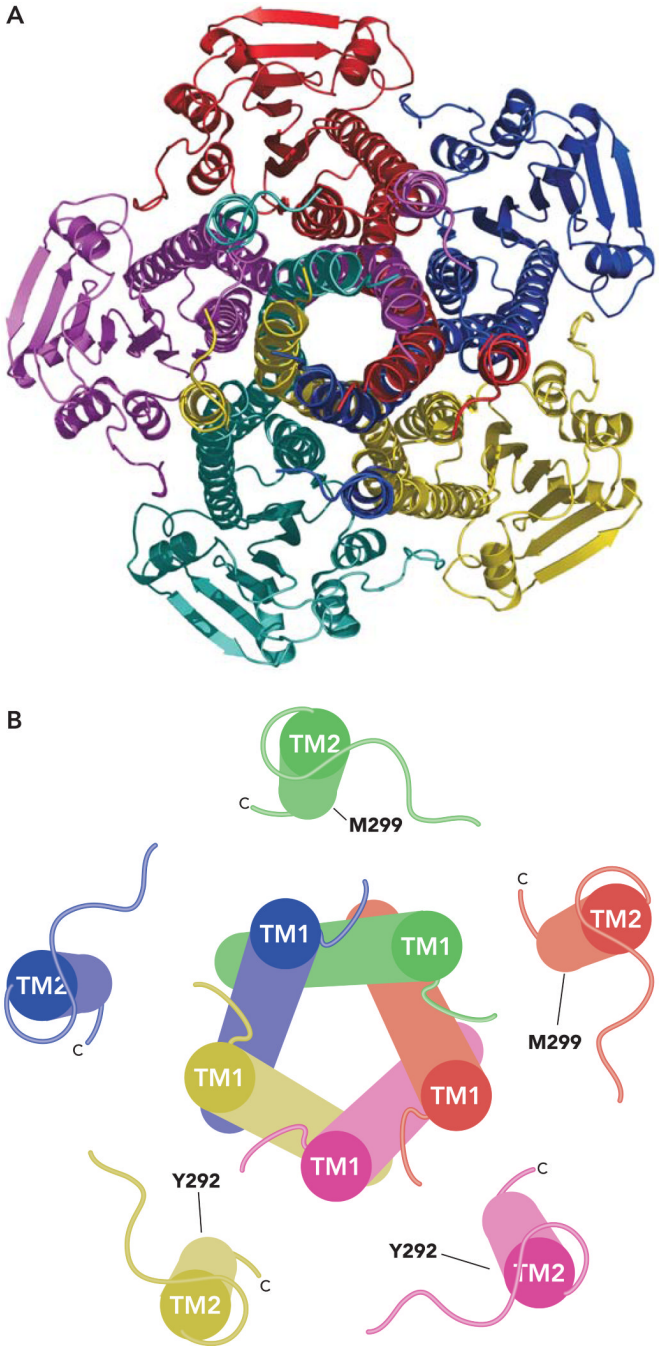

FIGURE 3. CorA membrane domain

A: CorA as seen from the periplasm. The CorA pentamer is shown from outside the cell looking down the pore, which is formed by TM1 in this closed form. Each monomer is colored differently. The five TM2 helices lie outside this pore, approximately 15 Å from the adjacent TM1 and 23 Å from another TM2. *B*: CorA membrane domain as cylinders. TM1 and TM2 are shown as cylinders with each monomer colored differently. The view is from the periplasm. Each TM2 is approximately perpendicular to the membrane, whereas each TM1 is angled slightly. Y292 near the periplasmic end of TM2 and M299 near the cytosolic end of TM2 are indicated on two monomers each. Cysteine substitution at either of these residues results in a pentamer containing five cysteines within the membrane. It is of interest that Y292C can

spontaneously cross-link to another Y292C residue. CorA carrying the M299C substitution does not spontaneously cross-link via a disulfide bond, but it can be induced to do so with copper-phenanthroline oxidation (71). Since each TM2 is 23 <ang from the adjacent TM2, these data strongly suggest that the TM2 helices must move in toward the apparent TM1 pore at some point during flux of Mg^{2+}.

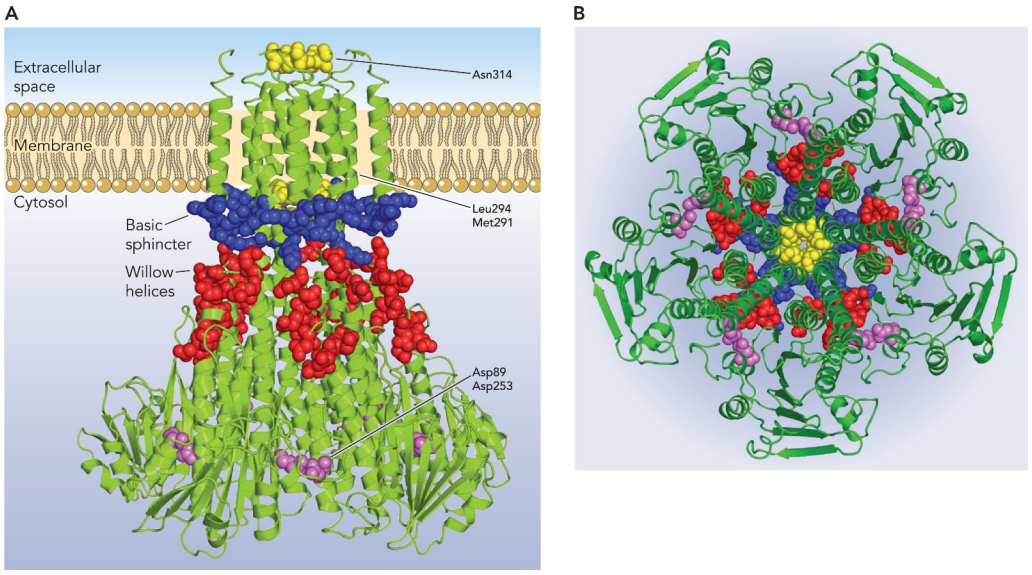

FIGURE 4. Important residues of the CorA Mg^{2+} channel

A: a view of the *T. maritima* Mg^{2+} channel from the side. Monomers are all in green. Potentially important residues are represented in space-filling form. The yellow residues are those within the pore formed by TM1 (N314, L294, M292) that appear to block the pore in its closed state. The blue residues are the lysines of the basic sphincter. The red residues are the aspartate and glutamate residues in the membrane proximal halves of the willow helices (α_5 and α_6). The lavender residues are the aspartate residues (D89 and D253) that bind Mg^{2+} between each monomer, apparently helping to hold the αβα domain of one monomer to the α_7 stalk helix of an adjacent monomer. *B*: a view of the *T. maritima* Mg^{2+} channel from the cytosol. The CorA channel is viewed down the funnel toward the membrane. Residues are colored as in part A but without labels.

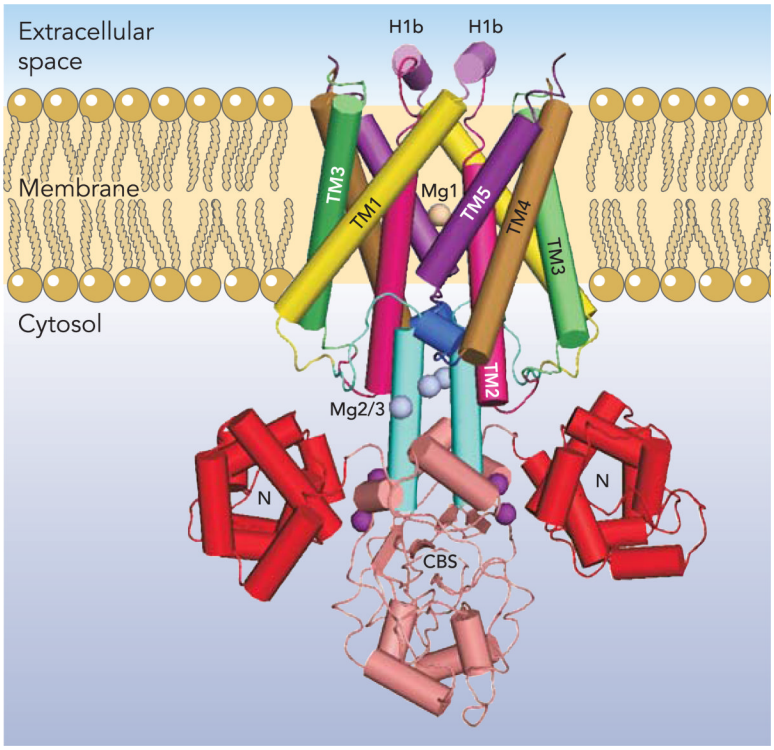

FIGURE 5. The MgtE Mg^{2+} channel

Structure of MgtE from *T. thermophilus*. MgtE is shown with each dimer colored identically. The N domain is shown in red, the CBS domains in beige, and the connecting helices in blue. Each of the TM segments of each monomer are shown in different colors and labeled. The H1b helices at the extracellular membrane face are shown in purple. Bound Mg^{2+} ions are labeled as follows: Mg1 within the pore is in wheat, Mg2 and Mg3 are in gray, and Mg4 and Mg5 are in purple. One of the Mg2 residues is obscured in this view.

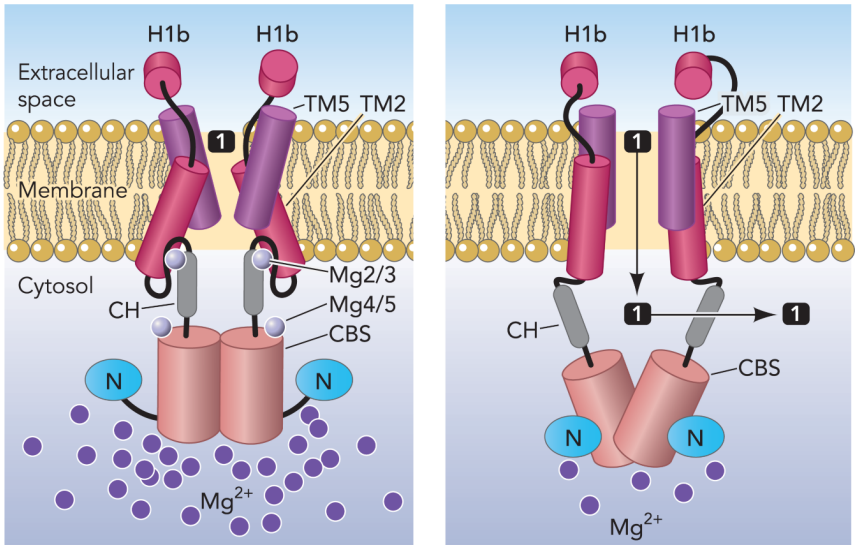

FIGURE 6. Cartoon structure of MgtE showing proposed domain movements during Mg^{2+} flux

This drawing is based on the model shown in Fig. 4, *C* and *D*, of Hattori et al. (20). The bound Mg^{2+} ions are shown as numbered light gray circles, whereas the additional light purple circles in the cytosol represent relative concentration of cytosolic free Mg^{2+}. The various domains are labeled as in previous figures. At *left*, Mg2/3 and Mg4/5 hold the CH to the TM domain and the N to the CBS domain, respectively. However, as cytosolic Mg^{2+} decreases, these bound Mg^{2+} ions may dissociate from MgtE. Loss of Mg2/3 would free the connecting helices from the TM domain, putatively allowing TM2 to move outward, changing the angle of TM5 relative to the membrane (*right*). Concomitantly, the loss of Mg4/5 would allow the N domain to swing out markedly, pulling the CBS domains apart, which in turn separates the connecting helices opening the pore for entry of Mg1 represented by the black square.

Table 1

Prokaryotic and eukaryotic Mg^{2+} transporters

Superfamily	Identified Members	Apparent Km for Mg^{2+}	Type of Transporter	References
CorA	**CorA,** ALR1/ALR2, Mrs2/ AtMrs2, Lpe10	**~ 15 μM**	**Channel,** Channels	22,23,66,67
MgtE	**MgtE,** SLC41A1, SLC41A2	0.7 mM, 0.3 mM	**Channel,** Carriers	65,75,13,14,54
TRPM	TRPM6 TRPM7 (LTRPC7, TRP-PLIK)		Channel/kinase (Chanzyme)	1,5,57,58,76, 42,43,59
Claudins	Claudin-16 (Paracellin-1) Claudin-19		Claudins	62
ACDP	ACDP2 (CNNM2)	0.6 mM	Putative channel	12
MagT1	MagT1	0.2 mM	Putative channel	15
Mgt	**MgtA, MgtB**	**10 μM**	**P-type ATPases**	64,66,69
NIPA1	NIPA1(SPG6)	0.7 mM	Putative channel	12
MMgT	MMgT1, MMgT2	1.5 mM, 0.6 mM	Putative channels	16

Text in **bold** denotes prokaryotic origin. Text in regular font denotes eukaryotic origin.